Journal of Power Sources 195 (2010) 516–521

Contents lists available at ScienceDirect

Journal of Power Sources

journal homepage: www.elsevier.com/locate/jpowsour

Short communication

Performance of a novel type of electrolyte-supported solid oxide fuel cell with honeycomb structure

Juan Carlos Ruiz-Morales[a,*], David Marrero-López[b], Juan Peña-Martínez[c], Jesús Canales-Vázquez[c], Joan Josep Roa[d], Mercè Segarra[d], Stanislav N. Savvin[a], Pedro Núñez[a]

[a] Departmento de Química Inorgánica, Universidad de La Laguna, 38200 Tenerife, Spain
[b] Departamento de Física Aplicada I, Universidad de Málaga, 29071 Málaga, Spain
[c] Instituto de Energías Renovables-Universidad de Castilla la Mancha, 02006 Albacete, Spain
[d] DIOPMA, Departamento de Ciencia de los Materiales e Ing. Metalúrgica, 08028 Barcelona, Spain

ARTICLE INFO

Article history:
Received 17 April 2009
Received in revised form 26 June 2009
Accepted 8 August 2009
Available online 15 August 2009

Keywords:
SOFC
Honeycomb structure
Hexagonal cells
NiO–YSZ composite

ABSTRACT

A novel design, alternative to the conventional electrolyte-supported solid oxide fuel cell (SOFC) is presented. In this new design, a honeycomb-electrolyte is fabricated from hexagonal cells, providing high mechanical strength to the whole structure and supporting the thin layer used as electrolyte of a SOFC. This new design allows a reduction of ~70% of the electrolyte material and it renders modest performances over 320 mW cm^{-2} but high volumetric power densities, i.e. 1.22 W cm^{-3} under pure CH_4 at 900 °C, with a high OCV of 1.13 V, using the standard Ni–YSZ cermet as anode, Pt as cathode material and air as the oxidant gas.

1. Introduction

Solid oxide fuel cells (SOFCs) are one of the alternative technologies for the production of clean energy, promising higher efficiencies and lower environmental impact.

Each assembled SOFC stack comprises several elements: electrolyte, anode, cathode, interconnect and sealing materials. The election of an appropriate candidate material for each component depends on its physical and chemical properties, which in turn largely control the cell performance. Among them, the reduction of the electrolyte thickness has been traditionally considered an important factor to achieve higher power densities. The thinner the electrolyte used, the better SOFC performance should be expected, as the latter is a reciprocal function of the ohmic resistance [1]. However, the decrease of the electrolyte thickness is limited to a value of about 150 μm [2], below which the SOFC becomes very fragile. In these cases, alternative cell designs, known as metal- or electrode-supported SOFC, are used. In these configurations, a 0.5–1.5 mm thick porous anode/cathode/metal supports the thin electrolyte layer (<150 μm) allowing the production of robust fuel cells. Nevertheless, one may find high performance of assembled SOFCs with thinner supported YSZ electrolytes (<20 μm) and/or thinner supporting substrates (250 μm from Topsoe Fuel Cells; 200–500 μm, CeramTec).

The main drawback in some of these designs is the rather large consumption of the electrode-supporting material, which turns out to be ineffective given that the extension of the Triple Phase Boundary (the layer where the electrochemical reactions take place) is usually restricted to a distance of 20–50 μm away from the electrolyte surface [3,4].

Here we report a procedure to produce electrolyte-supported SOFCs of novel design where ~100 μm thick electrolyte layers are produced. The mechanical strength is provided by a 2.0 mm thick layer of honeycomb yttria-stabilized zirconia (YSZ) which acts as a support of the thin electrolyte layer. The honeycomb structure is covered with a thin layer (10–20 μm) of the active anode material. This design has three important advantages over the traditional *state-of-the-art* configuration:

(1) It allows production of robust SOFCs with thin layers of electrolyte.
(2) It saves up to ~70% of the supporting (electrolyte or electrode) material, which will eventually lead to a drastic decrease of the cost of any stack assembled in this configuration. This opens the possibility of the fabrication of SOFC devices with a very high ratio of kW per cm^3 and/or kW per kg.

* Corresponding author at: Avda. Astrofísico Francisco Sánchez s/n, La Laguna, CP: 38200 Tenerife, Spain. Tel.: +34 922 31 84 64; fax: +34 922 31 84 61.
E-mail address: jcruiz@ull.es (J.C. Ruiz-Morales).

0378-7753/$ – see front matter © 2009 Elsevier B.V. All rights reserved.
doi:10.1016/j.jpowsour.2009.08.017

(3) It offers the possibility to fabricate a current collector (saving extra cost when using noble metals) at the external borders of the honeycomb structure, thus preventing the diffusion of the current collector material through the electrode microstructure and occlusion of the pores.

2. Experimental procedure

2.1. Materials

NOMEX honeycomb mesh (Goodfellow, UK); 8 mol% YSZ (PI-KEM, Staffordshire, UK); NiO (Sigma–Aldrich, Madrid, Spain, 99%); Pt-ink (Metalor Technologies, London, UK); methyl-ethyl-ketone, triton-Q, polyethyleneglycol PEG400, dibutyl phtalate, Butvar polyvinyl butyral (Sigma–Aldrich, Madrid, Spain). Mylar substrate film (Richard E. Mistler Inc., USA); cement-based sealing (Ceramabond 552-VFG and 552-VFG-T, Aremco Products Inc., NY).

2.2. Slurry preparation

A recently reported procedure [5] was followed in this work to prepare slurries except for a few changes made in the (ceramic powder:solvent) ratios.

The YSZ slurries were obtained by mixing the following materials: 10 g of YSZ, 10 g of a mixture of methyl-ethyl-ketone and ethanol (3:2, w/w) solvents; 0.5 g of Triton-Q (dispersant); 0.75 g of polyethylenglycol PEG400 (plasticiser); 0.75 g of dibutyl phthalate DBP (plasticiser) and 1 g of Butvar polyvinyl butyral PVB (binder). In the case of YSZ–NiO composites 6 g of NiO and 4 g of YSZ were dispersed in 13 g of methyl-ethyl-ketone:ethanol (3:2, w/w). The other components were added to the resulting dispersion in the same ratio considered for the YSZ slurry. In all cases, the components were ball-milled for 2 h at 150 rpm in a zirconia vessel with zirconia balls.

2.3. Fuel cell tests

Fuel cell tests were performed in a two-electrode arrangement [6], Fig. 1, using humidified 5%H_2 + 95%Ar gas mixture, pure H_2 or pure CH_4 as fuels and air as an oxidant. The cell was fixed to an alumina ring by a cement-based material (Ceramabond 552) and the whole sample was sealed to the fuel cell setup with the same cement, Fig. 1. *I–V* plots were recorded at a scan rate of 4 m Vs^{-1}, using a Zahner IM6e electrochemical workstation. Fuel gases were humidified by bubbling through a gas-washer thermostated at 20 °C to ensure a constant water content of 2.3%.

2.4. Characterisation of the YSZ mechanical properties

The picoindentation technique was performed by a MFP 3D (Asylum Research, Santa Barbara, CA) equipped with a SiO_2 tip of 10 nm constant radius (ACT-W, AppNano, Santa Clara, CA). The experiments were performed on the longitudinal and transversal surface by applying a load of 450 nN to operate within the elastic deformation range. The Young's modulus has been obtained by using Hertz equations [7].

2.5. Microstructural characterisation

Optical images of the cross-section and top-view of the samples were acquired using a stereomicroscope (Leica Zoom 2000, Leica Microsystems Inc., NY). Scanning electron microscopy images were obtained on a scanning electron microscope (Jeol JSM-6300, Tokyo, Japan). Prior to recording the images, the samples were cut and a fine gold layer was sputtered over the cross-sections to avoid charging-up.

3. Results and discussions

It is well known that the honeycomb arrangement provides mechanical strength to any supported structure due to an effective distribution of the load. Several materials with the aforementioned arrangement are commercially available, and among them, NOMEX mesh, Fig. 2(a). This material manufactured by DUPONT™, is mainly made of meta-aramid fibers and it exhibits several interesting properties, e.g. resistance to high temperatures. One may take advantage of this property to mold a ceramic-based material (e.g. YSZ) and create a backbone with hexagonal cells in a honeycomb structure, Fig. 2(b–d).

3.1. Fabrication of the honeycomb-structured materials with hexagonal cells

A piece of NOMEX mesh was coated with the slurry containing SOFC electrolyte material, in our case YSZ. This procedure resulted in the deposition of a thin plastic-like layer covering the honeycomb structure. Drying the green body at 200 °C for 1 h resulted in the production of a rigid structure, which could be easily manipulated, e.g. cut into small pieces of circular shape or perforated to create small holes to facilitate introduction of wire connections. Typically the process of coating and further drying at 200 °C was performed at least 3 times to produce an array of hexagonal honeycomb cells with final wall thickness ranging between 150 and 250 μm. As a final step, the rigid non-sintered assembly was fired at 1400 °C for 2 h, in order to remove all organic components and produce a dense ceramic material, preserving the hexagonal microstructure of the original NOMEX mesh, Fig. 2(c and d).

3.2. Fabrication of the electrolyte-supported SOFC with honeycomb structure

Several routes to fabricate the aforementioned structure were attempted. Firstly, the freshly coated NOMEX mesh was left to dry (at room temperature) on a Mylar substrate film. This approach resulted in the slight expansion of the electrolyte material at the bottom part of the coated NOMEX mesh. After drying at room temperature, the sample was removed from the Mylar substrate and further dried at 200 °C for 1 h. Several cycles of this procedure led to the closure of one side of the hexagonal cells as can be observed in Fig. 2(d) and more clearly in Fig. 3(a). The second route, which yielded the same result, consisted of attaching a thin layer of YSZ prepared by tape-casting [8] to one side of the YSZ-coated NOMEX mesh and co-firing the assembly to produce the supported structure. Slow ramp rates (1 °C min^{-1}) were used in this case to avoid cracks in the thin YSZ layer. Finally, the structure was fired at 1400 °C for 2 h. As can be seen in the cross-section of a single hexagonal cell, Fig. 3(a), the electrolyte is approximately 100 μm thick, the wall being thicker at the top of the cell. The upper part of the cell is fully dense, Fig. 3(b), as expected for the electrolyte functional layer, which is supposed to prevent mixing the oxidant and fuel gases.

The next step was the deposition of an anode layer by using a slurry of the *state-of-the-art* SOFC anode material (Ni/YSZ cermet) [9] to coat the inner part of the honeycomb structure, prior to final firing at high temperature, Fig. 3(c). As can be seen in Fig. 3(d) a thin (~20 μm) and porous layer of NiO–YSZ (60:40, wt%) covers the whole inner part of the hexagonal cells. The distribution of the anode porosity is especially good and may be increased under reducing conditions due to reduction of NiO to metallic Ni.

The last element of the fuel cell attached was the cathode material [10]. In our case, for testing purposes, a thin layer of Pt was

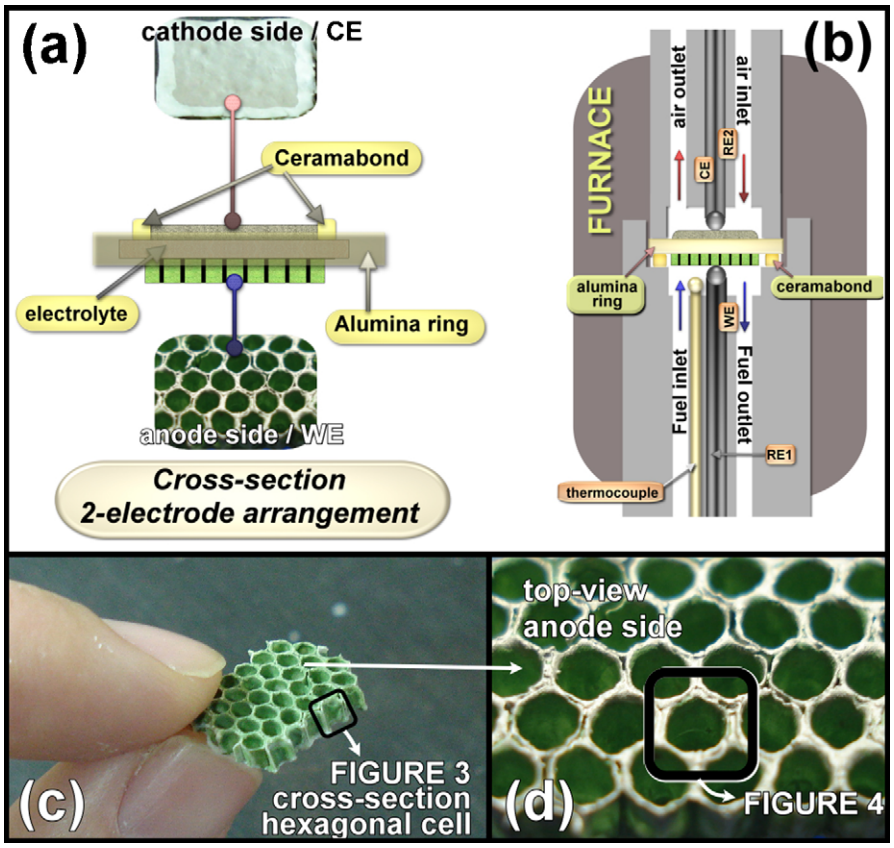

Fig. 1. (a) Schematic representation of the assembled fuel cell. (b) 2-point setup for fuel cell tests (WE: working electrode, CE: counter electrode and RE: reference electrode). (c and d) Scheme of the assembled fuel cell anode side showing the zones selected for Figs. 3 and 4.

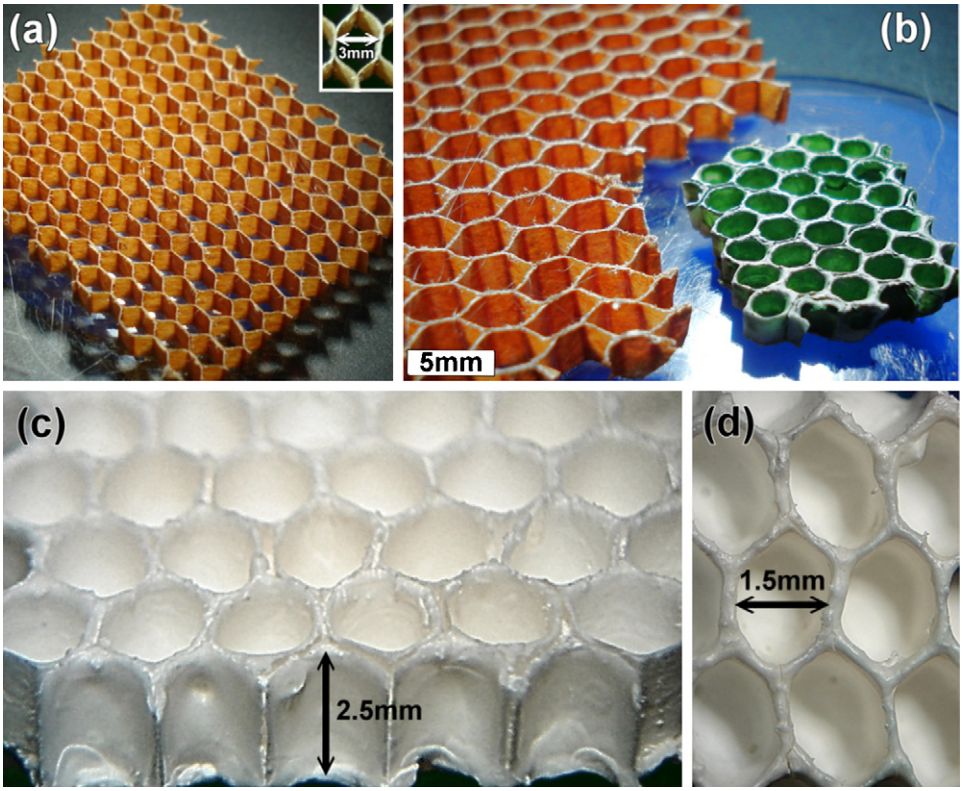

Fig. 2. (a) NOMEX honeycomb mesh with hexagonal 3 mm wide cells (inset). (b) Comparison of the size of a piece of NOMEX mesh and a sintered material produced with the honeycomb pattern. The molded material has a YSZ-backbone covered with a thin layer of NiO–YSZ composite. (c and d) Side- and top-view of a honeycomb YSZ-backbone molded with NOMEX honeycomb mesh. (d) The structure has a dense thin layer of YSZ covering one of the sides.

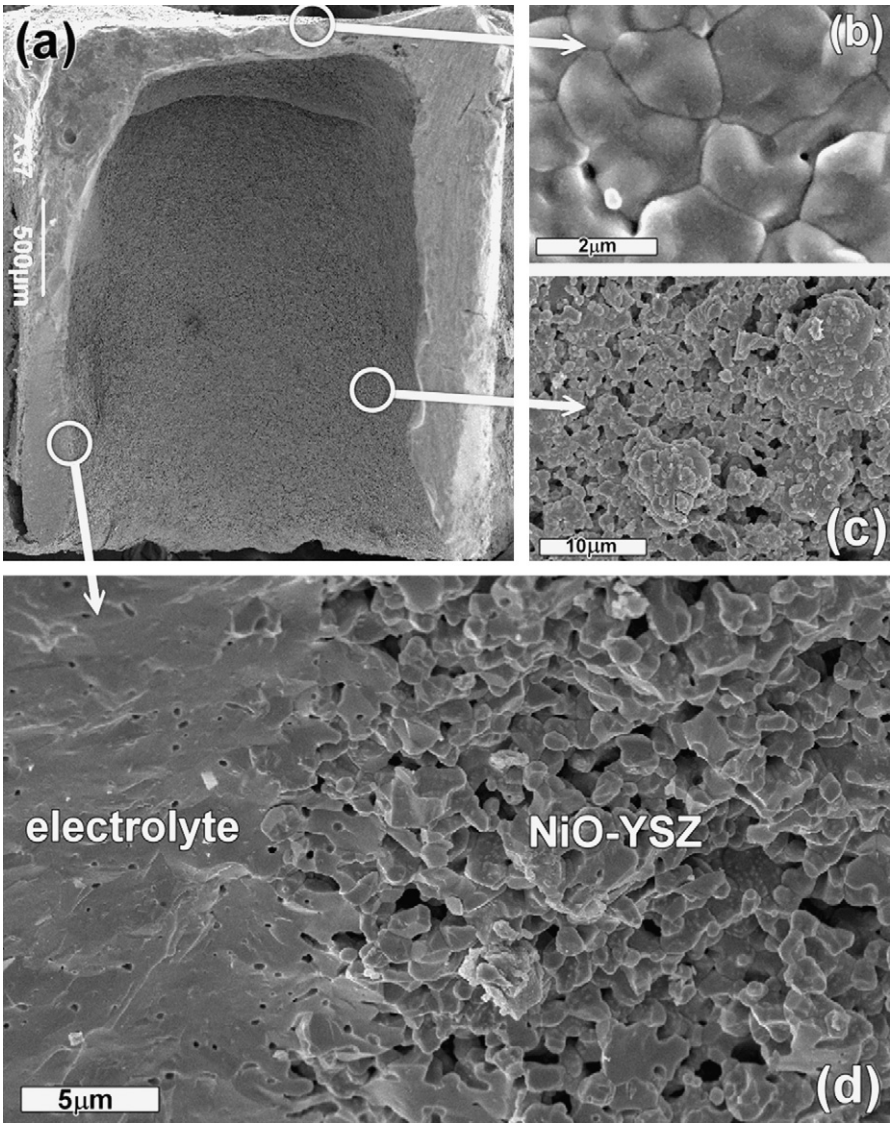

Fig. 3. (a) Cross-section SEM image of an individual YSZ hexagonal cell, supporting a ~100 μm thin YSZ layer. (b) Image of the supported YSZ layer (working as electrolyte in a SOFC), exhibiting full density with an average grain size ~3 μm. (c) SEM image showing the porous morphology of the NiO–YSZ composite in the inner part of each hexagonal cell. (d) Cross-section of a wall in one of the individual cells showing a homogeneous and porous 20 μm layer of NiO–YSZ (60:40, wt%) composite and a very good contact with the YSZ electrolyte.

deposited, which functioned simultaneously as a cathode and a current collector. Finally, a Pt current collector was deposited at the anode side after firing at 900 °C for 30 min. As mentioned in the introduction, the honeycomb design allows placing a layer of the current collecting material on the edge of each of the hexagonal cells, Fig. 4(a), saving Pt, which is typically deposited over the whole anode surface. As one may observe in Fig. 4(b) the Pt current collector is porous after firing under oxidising conditions.

Additionally, the hexagonal cells may be impregnated with different catalyst materials to improve the overall response of the anode. An example is shown in Fig. 4(c and d). In this case, a solution of $Ce(NO_3)_3{\cdot}6H_2O$ with dispersed 400 nm microspheres of poly(methyl methacrylate) (PMMA), Fig. 4(c), as pore formers was used to impregnate the inner part of each hexagonal cell. After firing, a layer of nanoparticles of CeO_2, a well-known catalyst for hydrocarbon oxidation, was obtained.

3.3. Mechanical tests

Two types of studies were performed to characterise the mechanical properties of the proposed configuration. In one of them, the AFM-FS technique was used to estimate the Young's modulus of YSZ. The value obtained of 190 ± 4.5 GPa was the same for both surfaces studied (longitudinal and transverse). This value is in agreement with the Young's modulus reported by Xie et al. [11], Wang et al. [12] and Selçuk and Atkinson [13]. This reveals that the fabrication process did not affect to the mechanical properties of the YSZ. In the other study, for the whole honeycomb-based assembly the critical load obtained was 2086 N and the critical rupture tension was estimated in 37.2 MPa. This value is rather low compared to the typical values of anode-supported SOFCs, i.e. 60–80 MPa. However, one should keep in mind that the supporting structure proposed has 70% less of material that the common anode-supported structures and hence the strength should be compared with very porous anode-supported cells. In those cases, very low values have been reported (<20 MPa) [14,15] or predicted [16].

3.4. Fuel cell tests

Fuel cell tests were performed with an assembled cell, which had geometrical area of 0.68 cm^2 and total thickness of ~2.5 mm. The thickness of the electrolyte layer was ~100 μm. The above (geomet-

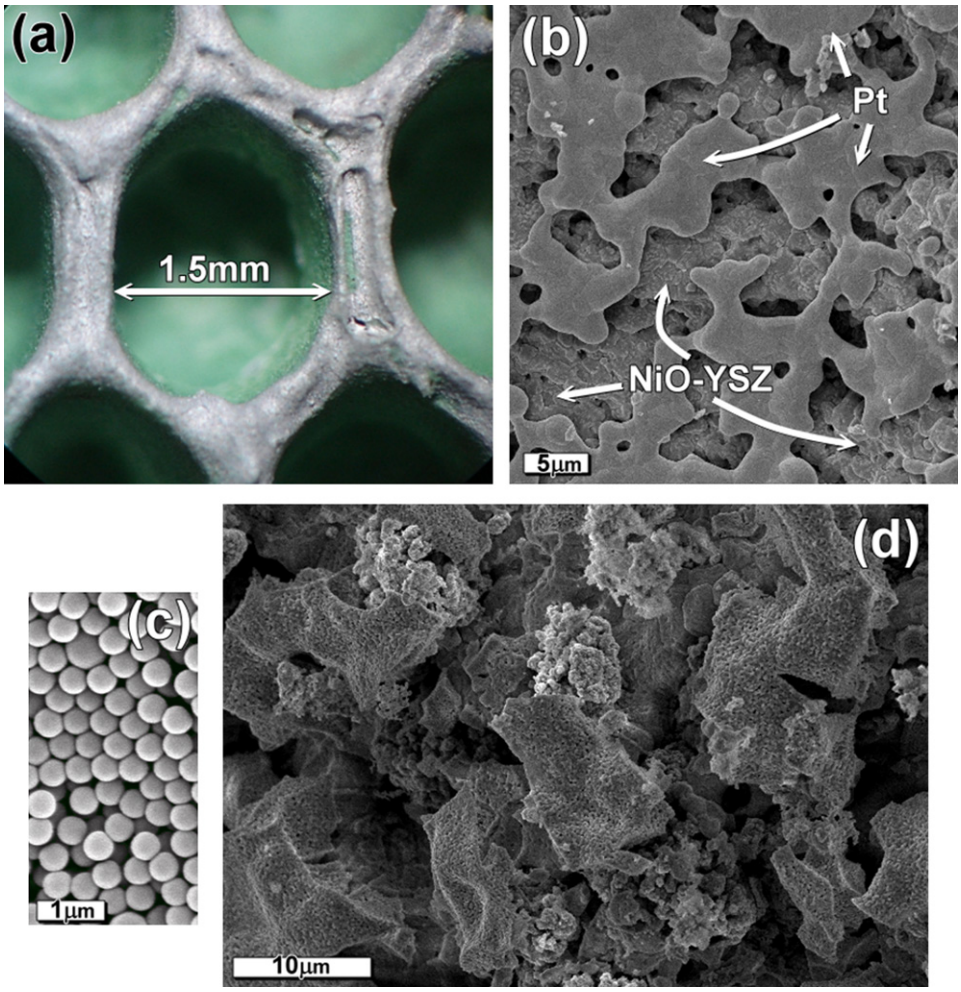

Fig. 4. (a) Top-view of a YSZ-honeycomb-hexagonal-cell covered with ~20 μm layer of NiO–YSZ (60:40, wt%). The edge of each cell has been painted with Pt paste. (b) The porous structure of the Pt layer, at the edges, after firing at 900 °C for 30 min. (c) PMMA 400 nm microspheres to produce a CeO_2 thin layer (d) after firing at 900 °C.

rical) area value was used to calculate the power density, rendering performances over 200 mW cm^{-2} and 320 mW cm^{-2} and stable cell OCV readings of 1.09 V and 1.13 V, under humidified pure H_2 and pure CH_4, respectively, at 900 °C, Fig. 5. However, evidence of carbon deposition was found after the test. The use of higher steam ratios in the fuel gas flow or lowering the working temperature would suppress the cracking reaction [1].

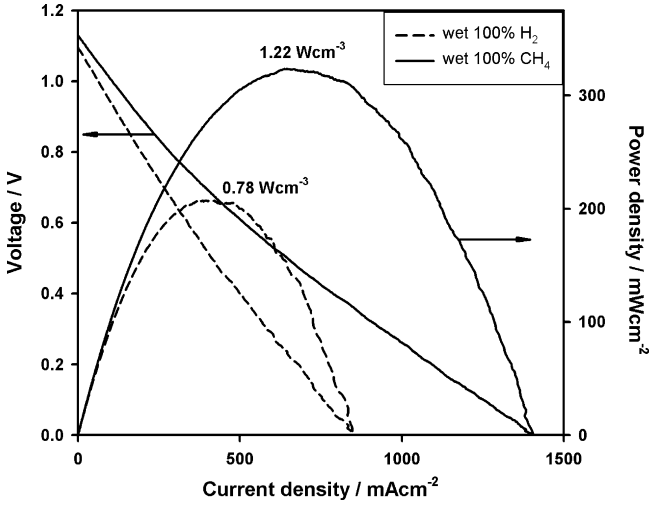

Fig. 5. Fuel cell test of an assembled honeycomb SOFC, at 900 °C, using humidified pure H_2 and CH_4 as fuel, and air as oxidant.

As can be observed the performance under CH_4 is higher than under H_2. One of the reasons for such a difference is that the OCV under methane is higher than in hydrogen. In this case, higher fuel cells performances could be expected.

Using an approximation [10] for the performance (P) expected in a SOFC:

$$P \approx \frac{\mathrm{OCV}^2}{4 \cdot (R^{\mathrm{ohmic}}_{\mathrm{electrolyte}} + R^{\mathrm{ohmic}}_{\mathrm{anode}} + R^{\mathrm{ohmic}}_{\mathrm{cathode}} + R^{\mathrm{polarisation}}_{\mathrm{anode}} + R^{\mathrm{polarisation}}_{\mathrm{cathode}})} \quad (1)$$

If the polarisation resistances in both fuels are negligible compared with the other contributions (which it is especially true at high temperature and thinner electrolytes), then, the ratio of performance under CH_4 and H_2 will be approximately:

$$\frac{P_{\mathrm{CH_4}}}{P_{\mathrm{H_2}}} \approx \left(\frac{\mathrm{OCV}_{\mathrm{CH_4}}}{\mathrm{OCV}_{\mathrm{H_2}}}\right)^2 \quad (2)$$

Hence from (Eq. (2)) one can expect higher performances with CH_4 if the OCV is higher than in H_2. For instance, if an OCV value of 1.2 V is used for CH_4 and 1.1 V for H_2, the ratio between perfor-

mances will be:

$$\frac{P_{CH_4}}{P_{H_2}} \approx \left(\frac{1.2}{1.1}\right)^2 \approx 1.19 \quad (3)$$

100 mV of difference between OCVs can lead to ~20% of the improvement in the overall efficiency (this is less relevant at lower temperatures, given that the OCV in H_2 increases with the temperature and in CH_4 decreases with the temperature).

This explains in part the observed performance, though in our case there is an additional and more significant effect. We think that the observed C-deposition helps to improve greatly the electrical contact between anode grains leading to an effective increase in the Triple Phase Boundary (TPB) and hence increasing the performance [17].

It should be mentioned that in our estimates of the power density we used the geometrical (cathode) surface area; yet one could expect larger active area values due to the complex shape of the anode compartment, which is extended away from its closed "flat" end along the walls of each hexagonal chamber up to the external current collector. Nevertheless, the evaluation of the active area is not a straightforward task in this case because the cathode and the anode electro-catalytically active sites are unevenly distributed, the latter being located in the honeycomb walls. Additionally, different contributions to the total ohmic resistance of the fuel cell can also be expected (this contribution can be minimised if the YSZ-honeycomb backbone is replaced by a NiO–YSZ composite). Therefore, a volumetric power density may be used to take into account the complex three-dimensional structure of the assembled SOFC. Therefore, values of 0.78 and 1.22 W cm^{-3} were obtained for the fuel cells operating at 900 °C and fed by humidified pure H_2 and CH_4, respectively.

The performance obtained under H_2-feed, 200 mW cm^{-2}, can be considered as rather modest compared with some values reported in excess of 1 W cm^{-2}. Nonetheless, from (Eq. (1)) one can estimate the maximum power density expected, taking into account, the OCV under pure H_2, the conductivity of the YSZ, the polarisation resistance of Pt under air with YSZ electrolyte (~0.35 Ω cm^2) and a negligible polarisation resistance of the Ni–YSZ anode under H_2, all these values at 900 °C.

This leads to a maximum power density of ~625 mW cm^{-2}. Hence, our value is just a 30% of the maximum value expected. The main limiting factor being the cathode overpotential (about 70% of the overall value). The other important factor, as mentioned before, is the different contributions to the total ohmic resistance from the YSZ-honeycomb backbone.

Other alternatives to the honeycomb-based structures have been proposed by several groups [18,19]. Basically, it is like comparing flat (our design) and tubular-like SOFC designs [18,19]. The tubular-like honeycomb structures [18,19] show high volumetric power densities and simple sealing process, but low kW per kg may be expected; in addition, no data under hydrocarbon-fed seems to be available. In our proposed design, a significant reduction of the supporting material is expected (70%), high volumetric power densities and high kW per kg can also be predicted in addition to high OCV with hydrocarbon-fed. However, there are also several drawbacks, the most important are the low mechanical strength and problems related to sealing.

With the ongoing work, we expect to improve the efficiencies of these devices by using perovskite-based cathodes such as LSM, thinner NOMEX mesh (500 μm) and/or a NiO–YSZ based composite for the coating procedure of the NOMEX mesh for decreasing the ohmic contribution of the supporting layer. The idea behind is to obtain the same performances but at temperatures below 700 °C.

4. Conclusions

To sum up, we have proposed an alternative design for the traditional electrolyte-supported SOFC. In this novel design a thin flat layer of YSZ is supported on a YSZ-honeycomb backbone with hexagonal cells. This configuration helps to improve the mechanical strength of the whole cell although it is still low, reduces fabrication costs due to lower electrolyte/electrode material consumption (~70% less) and provides performance of 320 mW cm^{-2} or 1.22 W cm^{-3} and an OCV of 1.13 V, at 900 °C, under humidified pure CH_4.

Acknowledgements

This work has been supported by Spanish Research Program, under Grant No. MAT2007-60127 and by the "Ministerio de Educación y Ciencia" through the programme "Ramón y Cajal" (J.C.R.-M.). The authors also acknowledge financial support from JCCM (PAC08-0183-9399).

References

[1] S.C. Singhal, K. Kendall, High Temperature Solid Oxide Fuel Cells, Elsevier, Oxford, UK, 2004.
[2] B.C.H. Steele, J. Mater. Sci. 36 (2001) 1053–1068.
[3] S. Primdahl, Nickel/yttria-stabilised zirconia cermet anodes for solid oxide fuel cells, Thesis, University of Twente, The Netherlands, 1999.
[4] A.J. Appleby, F.R. Foulkes, Fuel Cell Handbook, Van Nostrand Reinhold, New York, 1989.
[5] J.C. Ruiz-Morales, J. Peña-Martínez, J. Canales-Vázquez, D. Marrero-López, C. Savaniu, P. Núñez, J. Am. Ceram. Soc. 92 (1) (2009) 276–279.
[6] J.C. Ruiz-Morales, J. Canales-Vázquez, J. Peña-Martínez, D. Marrero-López, P. Núñez, Electrochim. Acta 52 (1) (2006) 278–284.
[7] H. Hertz, J. Reine, Angew. Math. 92 (1881) 156–171.
[8] R.E. Mistler, E.R. Twiname, Tape Casting: Theory and Practise, Wiley-American Ceramic Society, Westerville, OH, 2000.
[9] H.S. Spacill, U.S. Patent 3,558,360 (1970).
[10] N.Q. Minh, T. Takahashi, Science and Technology of Ceramic Fuel Cells, Elsevier, Amsterdam, 1995.
[11] Y. Xie, X. Zhang, M. Robertson, R. Maric, D. Ghosh, J. Power Sources 162 (2006) 436–443.
[12] Y. Wang, K. Duncan, E.D. Wachsman, F. Ebrahimi, Solid State Ionics 178 (2007) 53–58.
[13] A. Selçuk, A. Atkinson, J. Eur. Ceram. Soc. 17 (1997) 1523–1532.
[14] J.H. Yu, G.W. Park, S. Lee, S.K. Woo, J. Power Sources 163 (2007) 926–932.
[15] G. Matula, T. Jardiel, R. Jimenez, B. Levenfeld, A. Várez, Arch. Mater. Sci. Eng. 32 (1) (2008) 21–25.
[16] M. Radovic, E. Lara-Curzio, Acta Mater. 52 (2004) 5747–5756.
[17] S. McIntosh, H. He, S.-I. Lee, O. Costa-Nunes, V.V. Krishnan, J.M. Vohs, R.J. Gorte, J. Electrochem. Soc. 151 (4) (2004) A604–A608.
[18] H. Zhong, H. Matsumoto, T. Ishihara, A. Toriyama, Solid State Ionics 179 (2008) 1474–1477.
[19] T. Yamaguchi, S. Shimizu, T. Suzuki, Y. Fujishiro, M. Awano, J. Am. Ceram. Soc. 92 (2009) S107–S111.